J. Hydrol. Hydromech., *59*, 2011, 3, 206–216
DOI: 10.2478/v10098-011-0017-5

NUMERICAL SIMULATION OF FLY-ASH TRANSPORT IN THREE SANDS OF DIFFERENT PARTICLE-SIZE DISTRIBUTIONS USING HYDRUS-1D

RADKA KODEŠOVÁ[1)], ALEŠ KAPIČKA[2)], JAKUB LEBEDA[1)], HANA GRISON[2)], MARTIN KOČÁREK[1)], EDUARD PETROVSKÝ[2)]

[1)]Department of Soil Science and Soil Protection, Czech University of Life Sciences Prague, Kamýcká 129, 165 21 Prague 6, Czech Republic; Mailto: kodesova@af.czu.cz
[2)]Institute of Geophysics, Academy of Sciences of the Czech Republic, Boční 1401, 141 31 Prague 4, Czech Republic.

Study is focused on the numerical modeling of fly-ash transport in three sands, which was experimentally studied in the laboratory. Sands were packed in glass cylinders with diameter of 5.52 cm and height of 18 cm. Sands were also packed in plastic cylinders with diameter of 30 cm and height of 40 cm. The fly-ash and pulse infiltrations were applied on the top of all cylinders. Visually observed and gravimetrically evaluated fly-ash migration in small cylinders corresponded to fly-ash mobility in large columns detected using the SM400 Kappameter. The HYDRUS-1D code was used to simulate observed fly-ash transport. Parameters of soil hydraulic functions were either obtained using the Tempe cells and the RETC program or estimated using numerical inversion of transient water flow data measured in both types of columns using HYDRUS-1D. Parameters characterizing colloid transport in sands were then estimated from the final fly-ash distribution in sandy columns using attachment/detachment concept in HYDRUS-1D. Fly-ash mobility increased with increasing sand particle sizes, e.g. pore sizes. Particle sizes and pore water velocity influenced the attachment coefficient, which was calculated assuming filtration theory. The same longitudinal dispersivity, sticking efficiency and detachment coefficient sufficiently characterized fly-ash behavior in all sands.

KEY WORDS: Sand, Fly-ash Migration, Magnetic Susceptibility, Numerical Simulation, Attachment/Detachment Concept, Filtration Theory.

Radka Kodešová, Aleš Kapička, Jakub Lebeda, Hana Grison, Martin Kočárek, Eduard Petrovský: NUMERICKÁ SIMULACE TRANSPORTU ÚLETOVÉHO POPÍLKU VE TŘECH PÍSCÍCH RŮZNÉHO ZRNITOSTNÍHO SLOŽENÍ POMOCÍ HYDRUS-1D. J. Hydrol. Hydromech., *59*, 3; 45 lit., 4 obr., 4 tab.

Studie je zaměřena na numerické modelování transportu úletového popílku ve třech píscích, který byl experimentálně studován v laboratoři. Písky byly nahutněny ve skleněných válcích o průměru 5,52 cm a výšce 18 cm. Písky byly také nahutněny v plastových válcích o průměru 30 cm a výšce 40 cm. Na povrchu válců byly aplikovány jednorázové infiltrace vody s popílkem. Migrace úletového popílku pozorovaná vizuálně a zjištěná gravimetricky v malých válcích odpovídala mobilitě úletového popílku detekované Kappametrem SM400 ve velkých válcích. Pozorovaný transport úletového popílku byl simulován programem HYDRUS-1D. Parametry hydraulických funkcí byly získány buď pomocí Tempských cel a programu RETC nebo odhadovány numerickou inverzí transientních data měřených na obou typech válců programem HYDRUS-1D. Parametry charakterizující transport koloidů v píscích byly potom odhadovány z konečné distribuce úletového popílku v písčitých sloupcích užitím konceptu attachment/detachment (připojení/odpojení) v programu HYDRUS-1D. Mobilita úletového popílku se zvyšovala se zvyšující se velikostí písčitých zrn, tj. s velikostí pórů. Velikost zrn a pórová rychlost ovlivnila depoziční (attachment) koeficient, který byl počítán na základě filtrační teorie. Stejné hodnoty podélné disperze, efektivity blokování (sticking efficiency) a mobilizačního (detachement) koeficientu charakterizovaly chování úletového popílku ve všech píscích.

KLÍČOVÁ SLOVA: písek, migrace úletového popílku, magnetická susceptibilita, numerická simulace, attachment/detachment koncept, filtrační teorie.

Introduction

Soil and water contamination due to atmospheric deposition is a serious environmental problem especially in the industrial regions. It was shown that magnetic measurements can serve as proxy of industrial immisions as well as heavy-metal contamination (*Petrovský* and *Elwood*, 1999; *Hanesch* et al., 2003; *Boyko* et al., 2004). The method is based on the fact that industrial fly-ashes contain about 10% of ferrimagnetic particles, namely Fe-oxides (*Flanders*, 1994; *Kapička* et al., 2001). Magnetic susceptibility of soils was mapped in surroundings of local sources of pollution (*Kapička* et al., 1999; *Hanesch* and *Scholger*, 2002; *Spiteri* et al., 2005; *Sharma* and *Tripathi*, 2007), or at regional to national scales (*Hay* et al., 1997; *Heller* et al., 1998; *Magiera* and *Strzyszcz*, 2000; *Kapička* et al., 2008). Ferrimagnetic particles are usually accumulated at the soil surface. However, they may be transferred into grater depths due to the soil tillage, erosion etc. In some soils (like sandy soils or soils with well developed and stable aggregates) particles may migrate within the soil profile.

The soil and groundwater contamination associated with the presence of suspended particles has recently attracted significant attention because of either harmfulness of colloid particles themselves or due to toxic substances adsorbed onto the colloidal particles. Colloid transport is studied in both the macroscopic and microscopic scales. Many studies have been done in microscale using the artificial micromodels to show single particles behavior in pores of specific shapes and under different pore saturation by water via monitoring of particle trajectories or their attachment to solid particles due to the small pore radius, pore blocking by colloids, attachments to other colloid particles, water film covered solid particles or water-air interfacial tension (*Sirivithayapakorn* and *Keller*, 2003; *Keller* et al., 2004; *Auset* and *Keller*, 2004). Colloid transport was also experimentally studied at macroscale, such as in laboratory studies of *Bolster* et al. (1999), *Bradford* et al. (2002), *Gargiulo* et al. (2007, 2008), *Torkzaban* et al. (2008), *Foppen* et al. (2010) and *Schinner* et al. (2010) who investigated bacteria mobility in porous columns, or in the field study *Wossner* et al. (2001) who evaluated the viral transport in sand and gravel aquifer.

Colloid transport may be mathematically simulated in microscale (*Gao* et al., 2010). Several mathematical models describing colloid transport in macroscale have been also designed (*Sim* and *Chrysikopulos*, 2000; *Bradford* et al., 2003; *Kim*, 2006). The conceptual model for colloid transport included in HYDRUS-1D code (Šimůnek et al., 2008) accounts for colloid attachment, straining and exclusion. The HYDRUS-1D code was successfully tested and results were presented by *Bradford* et al. (2003, 2004 and 2005), *Jiang* et al. (2010) or *Gargiulo* et al. (2007, 2008).

Fly-ash transport in porous media has not been previously studied. Fly-ash was usually used to change properties of original porous material. Among others *Zhang* et al. (2010) used fly-ash to increase phosphorus sorption in sand. In experimental and mathematical studies mentioned above the maximum colloid-size was 1 μm that is 10 times smaller then the average size of fly-ash particles. As showed by *Gargiulo* et al. (2007), bacteria (*R. rhodochrous*), transport of which was observed and simulated in tree sands, may create three-dimensional aggregates that can reach the size of 10–15 μm, while single cells have a diameter of only 0.8–1 μm. They suggested that tendency of this bacteria to form aggregates (similar size as the average size of fly-ash particle) enhanced their deposition in the porous material.

The main goals of this study were: 1. experimental evaluation of fly-ash mobility in three types of sands, 2. numerical evaluation of such size particles transport within the sand columns using the HYDRUS-1D code, 3. specification of sand vulnerability to fly-ash contamination depending on soil particle-size distribution.

Material and methods

Experimental data

Small columns

Three technical quartz sands (composition, is documented in thin section images, Fig. 1) from the sand mine Sklopísek Střeleč were used to study fly-ash mobility in porous media: ST8 (particle sizes 0.10–0.63 mm) – fine sand, ST03/08 (particle sizes 0.315–0.80 mm) – medium sand, and ST 06/12 (particle sizes 0.63–1.25) – coarse sand. Sands were packed in glass cylinders with diameter of 5.52 cm and heighs of 18 cm. Two grams of fly-ash and 100 cm^3 of distilled water were applied on the top of the sand columns (SGC1 run). Suspension infiltration and outflow at the column bottom was monitored. The typical breakthrough curve was not measured. The small column experiments were performed to

validate fly-ash distribution in large soil columns described using the magnetic susceptibility data (see below) and to obtain hydraulic and transport parameters under similar conditions. The fly-ash migration was assessed visually. Then the soil columns were divided into the 2 cm thick layers. Fly-ash was washed out from each sand layer by 100 cm^3 of distilled water and after that water was extracted using the evaporation table. The amount of fly-ash in each sand layer was determined gravimetrically. To eliminate possible impact of very fine particles presented in the sands, approximately the same amounts (3 replicates) as in each layer of clean sands were also washed by 100 cm^3 of distilled water and water was again extracted using the evaporation table. Detected amount of fine particles were subtracted from values determined for column layers. Fly ash content in soil column was expressed as a total fly-ash mass per unit of dry sand, m_t [M M^{-1}]. Experiments were repeated with the same amount of fly-ash, and 200 or 300 cm^3 of distilled water (SGC2 and SGC2 runs) (Tab. 1).

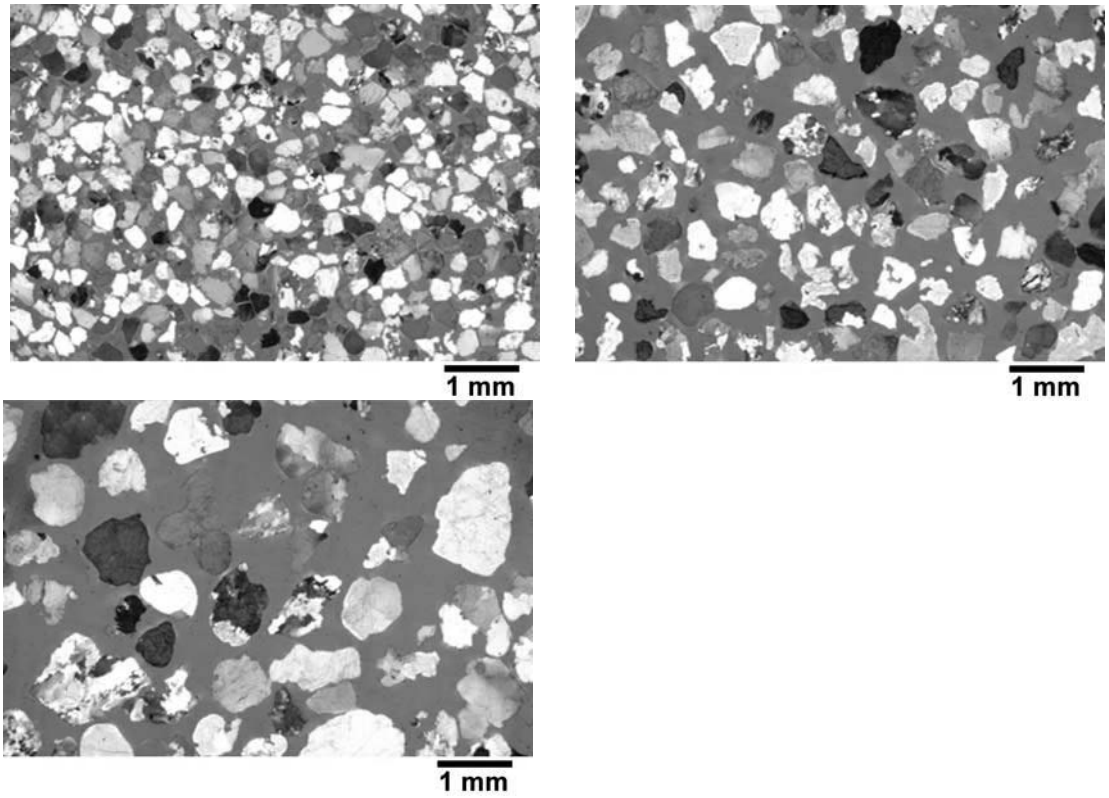

Fig. 1. Sand morphology and pore structure studied on micro-morphological images of fine (top left), medium (top right) and coarse (bottom) sands.

T a b l e 1. Characteristics of experiments performed in sands packed in small glass columns (SGC): inflow (Q_{inf}) and outflow (Q_{out}) volume, inflow (c_{inf}) and outflow (c_{out}) concentration, time of infiltration pulse (t_{inf}), time of outflow beginning ($t_{out,ini}$), total simulated time (t_{tot}).

Sand	Exp. run	Q_{inf} [cm^3]	c_{inf} [mg cm^{-3}]	t_{inf} [min]	Q_{out} [cm^3]	c_{out} [mg cm^{-3}]	$t_{out,ini}$ [min]	t_{tot} [min]
Fine ST 06/12	SGC1	100	20	0.40	0	–	–	5
	SGC2	200	10	1.37	45.9	0	1.07	5
	SGC3	300	6.7	2.78	145.4	0.123	1.05	5
Medium ST03/08	SGC1	100	20	0.19	0	–	–	3
	SGC2	200	10	0.52	67.0	0.111	0.47	3
	SGC3	300	6.7	1.12	167.7	0.077	0.43	3
Coarse ST8	SGC1	100	20	0.17	0	–	–	2
	SGC2	200	10	0.29	83.7	3.80	0.25	2
	SGC3	300	6.7	0.42	183.0	2.77	0.22	2

Large columns

Sands were also packed in plastic cylinders with diameter of 30 cm and height of 40 cm. The 5 cm coarse sand drainage layers were formed below the studied sand layers. The sensors SM200 (*Delta-T Devices Ltd.*, 2005) for soil-water content measurements and micro-tensiometers Tensior 5 (*UMS GmbH, Munich*, 2005) for pressure head measurements were placed 10, 20 and 30 cm below the sand surface to monitor water regime within the sand columns. The plastic tube for inserting the Kappameter SM400 (*Petrovský* at al., 2004) was positioned in the column center. The SM400 device, which measures vertical distribution of magnetic susceptibility, was used to monitor migration of the fly-ash ferrimagnetic particles. The water regime was initially studied on each soil column using the ponding infiltration (maximum ponding depth of 5 cm) on the column top. Three different fresh water infiltration pulses were applied in different experimental runs (LPC1, LPC2, LPC3) (Tab. 2). Next the fly-ash (emitted from Porici power plant) and fresh water was applied (LPC-FA run). Time intervals between experiments were 2 to 4 weeks to insure similar initial conditions. The applied fly-ash doses varied for different sands due to the sensitivity of the SM400 device. The applied fly-ash amount increased with expected increase of fly-ash mobility in each sand material: 50 g on the fine, 100 g on the medium and 150 g on the coarse sand. Water regime was monitored using the SM200 sensors and micro-tensiometers Tensior 5. The final magnetic susceptibility within the soil profile and consequently fly-ash distribution was measured when no significant water flow and consequently no fly-ash transport was observed.

T a b l e 2. Characteristics of experiments perform in sands packed in large plastic columns (LPC): inflow volume (Q_{inf}), inflow concentration (c_{inf}), time of infiltration pulse (t_{inf}), total simulated time (t_{tot}).

Sand	Exp. run	Q_{inf} [cm^3]	c_{inf} [mg cm^{-3}]	t_{inf} [min]	t_{tot} [min]
Fine ST 06/12	LPC1	4700	–	1.67	40
	LPC2	8910	–	3.88	60
	LPC3	15850	–	7.50	70
	LPC-FA	3700	13.51	1.31	20
Medium ST03/08	LPC1	5350	–	0.68	50
	LPC2	9780	–	1.28	60
	LPC3	10430	–	1.42	70
	LPC-FA	3120	32.05	0.40	10
Coarse ST8	LPC1	4950	–	0.35	30
	LPC2	16750	–	1.22	40
	LPC3	17110	–	1.25	75
	LPC-FA	2100	71.43	0.15	10

Numerical simulations
Theory

The HYDRUS-1D program (*Šimůnek* et al., 2008a,b) was applied to simulate water flow and fly-ash transport in sands. The Richards equation, which describes the one-dimensional isothermal Darcian flow in a variably saturated rigid porous medium, is used in this model. To solve this equation, the soil hydraulic properties must be specified. *The van Genuchten* (1980) analytical expressions are used to describe soil hydraulic functions, the soil water retention curve, $\theta(h)$, and the hydraulic conductivity function, $K(\theta)$:

$$\theta_e = \frac{\theta(h) - \theta_r}{\theta_s - \theta_r} = \frac{1}{\left(1 + |\alpha h|^n\right)^m}, \quad h < 0$$

$$\theta_e = 1, \quad h \geq 0 \tag{1}$$

$$K(\theta) = K_s\, \theta_e^l \left[1 - \left(1 - \theta_e^{1/m}\right)^m\right]^2, \quad h < 0$$

$$K(\theta) = K_s, \quad h \geq 0 \tag{2}$$

where θ is the soil water content [L^3 L^{-3}], θ_e – the effective soil water content [–], θ_r and θ_s are the residual and saturated soil water contents [L^3 L^{-3}], respectively, h – the pressure head [L], l – the pore-connectivity parameter [–], α – the reciprocal of the air-entry pressure head [L^{-1}], n [–] is related to the

slope of the retention curve at the inflection point, and $m = 1 - 1/n$, K – the hydraulic conductivity [L T^{-1}], K_s – the saturated hydraulic conductivity [L T^{-1}]. Parameters θ_r, θ_s, α, n and K_s must be known when simulating water regime.

A modified form of the advection-dispersion equation is employed in HYDRUS-1D to simulate virus, colloid, and bacteria transport assuming attachment/detachment concept. Mass transfer between the aqueous and solid phase is described using following equation:

$$\rho \frac{\partial s}{\partial t} = \theta k_a \psi c - k_d \rho s, \quad (3)$$

where c is the (colloid, virus, bacteria) concentration in the aqueous phase [M L^{-3}], s – the solid phase (colloid, virus, bacteria) concentration [M M^{-1}], ρ_d – the bulk density [M L^{-3}], k_a – the first-order deposition (attachment) coefficient [T^{-1}], k_d – the first-order entrainment (detachment) coefficient [T^{-1}], and ψ is a colloid retention function [–], which is function of the diameter of the sand grain, d_c [L], and coordinate. The attachment coefficient may be calculated using filtration theory as a function of the soil water content, diameter of the sand grains, d_c [L], diameter of the colloid particles, d_{co} [L], sticking efficiency, ζ [–], pore-water velocity v [L T^{-1}], and the single-collector efficiency, η [–]. Theory is in greater detail described in HYDRUS-1D manual (*Šimůnek* et al., 2008a). Parameters ρ_d, d_c, d_{co}, ζ, and k_d must be known when simulating colloid transport. In addition the longitudinal dispersivity, D_L [L], must be defined to solve the advection-dispersion equation.

Small columns

The water flow within the sand columns was initially numerically analyzed. Soil water retention curves were measured using the Tempe cells. Sands were packed into 100-cm^3 cylinders (soil core height of 5.1 cm and diameter of 5.0 cm) placed into the cells (3 replicates for each sand). Initially, fully saturated soil samples were slowly drained using six pressure head steps (–10, –30, –50, –100, –200 and −350 cm) during a 2-week period. Data points of soil water retention curve were evaluated using the final soil water content and water outflow monitored using byrettes. The RETC program (*van Genuchten* et al., 2005) was used to obtain θ_r, θ_s, α and n parameters of van Genuchten function (Tab. 3) by fitting data of all 3 replicates (which were very similar). Parameters θ_r were set at 0.01 cm^3 cm^{-3} in all cases. Parameter n was restricted to be maximally 3 (larger values caused computational instabilities when simulating some of following water and flay-ash transport scenarios). The saturated hydraulic conductivities, K_s, were estimated using numerical inversion of outflow data measured on small glass columns (SGC3 – infiltration pulse of 300 cm^3) using HYDRUS-1D. Initial conditions were set at low pressure head values of –500 cm corresponding to very dry conditions. Observed infiltration rates were used to specify the top boundary conditions. Seepage face boundary conditions were defined at the bottom.

Next, the fly-ash transport was simulated. The bulk density, ρ_d, diameters of the sand grains, d_c, and diameter of the colloid particles, d_{co}, were set to measured values (Tab. 4). The longitudinal dispersivity, D_L, sticking efficiency, ζ, and the detachment coefficient, k_d, were calibrated manually from the final fly-ash content, m_t, in soil columns. Since m_t values expressed the average total fly ash content in 2 cm thick sand layers, the corresponding information had to be computed from the simulated data (using final c, s and θ and ρ_d) to find the best fits. Concentration flux and zero concentration gradient were set at the top and bottom, respectively. Obtained soil hydraulic and fly-ash transport parameters were used to simulate water flow and fly-ash transport when infiltration pulses of 100 or 200 cm^3 were applied, to validate obtained results.

Large columns

The water flow within the sand columns was first analyzed numerically using the data from previous experiments. Since simulated water regime did not closely correspond to the monitored one, a new parameter optimization was performed. Parameter θ_r, θ_s and n were set to values obtained from the Tempe cells experiment (Tab. 3). The α and K_s values were estimated using numerical inversion of the soil water contents and pressure heads measured in the large plastic columns using HYDRUS-1D. Initial conditions were set at values measured at the beginning of each test. Observed infiltration rates were used to specify the top boundary conditions. Seepage face boundary conditions were defined at the bottom. Optimization was performed for three infiltration pulses (LPC1, LPC2, and LPC3).

Finally, parameters (Tab. 4), which were obtained on small columns to characterize fly-ash

transport, were used to simulate fly-ash behavior in the large columns under condition of LPC-FA run. A new optimization was not performed, because measured magnetic susceptibility data could not be directly related to fly-ash content within the sand columns (measurements were also impacted by water content, temperature etc., *Kapička* et al., 2011). In addition, measured values represented magnetic susceptibility integrated within the depth of approximately 2.5 cm, which made difficult to correctly analyze magnetic susceptibility at the column top. Two simulations were performed for each sand using either the soil hydraulic parameters used for simulating the small column scenarios or the average soil hydraulic parameters obtained from the large column data.

T a b l e 3. Van Genuchten soil hydraulic parameters obtained using the Tempe cells and the RETC program (small glass column – SGC), numerical inversion using the HYDRUS-1D program from small glass (SGC) or large plastic column (LPC).

Sand	Cylinder/Exp. run	θ_s [cm^3 cm^{-3}]	θ_r [cm^3 cm^{-3}]	α [cm^{-1}]	n [–]	K_s [cm min^{-1}]
Fine ST 06/12	SGC3	0.400	0.01	0.047	3	5.30
	LPC1	0.400	0.01	0.063	3	2.89
	LPC2	0.400	0.01	0.055	3	10.63
	LPC3	0.400	0.01	0.071	3	3.43
Medium ST03/08	SGC3	0.399	0.01	0.077	3	12.77
	LPC1	0.399	0.01	0.116	3	20.00
	LPC2	0.399	0.01	0.123	3	22.88
	LPC3	0.399	0.01	0.185	3	17.45
Coarse ST8	SGC3	0.399	0.01	0.094	3	29.95
	LPC1	0.399	0.01	0.190	3	31.91
	LPC2	0.399	0.01	0.178	3	24.85
	LPC3	0.399	0.01	0.203	3	30.45

T a b l e 4. Parameters used to simulate fly-ash migration in sands.

Sand	Bulk density [g cm^{-3}]	Longitudinal dispersivity [cm]	Sand particle diameter [cm]	Fly-ash particle diameter [cm]	Sticking efficiency [–]	First-order detachment coefficient [min^{-1}]
Fine ST 06/12	1.53	1.5	0.035	0.001	5	1.5
Medium ST03/08	1.54	1.5	0.056	0.001	5	1.5
Coarse ST8	1.56	1.5	0.093	0.001	5	1.5

Results and discussion

Small columns

The measured final fly-ash distributions in the sand columns packed in the small glass cylinders are shown in Fig. 2. The fly-ash recovery (sum of fly-ash content in sand and suspension discharge at the bottom) was 99.5, 99.7 and 94.9 % (fine sand), 95.2, 99.7 and 99.4 % (medium sand), and 92.5, 92.1 and 95.2 % (coarse sand) of applied dose, for 100, 200 and 300 cm^3 of distilled water, respectively. The fly-ash discharge at the bottom was 0, 0 and 0.9 % (fine sand), 0, 0.37 and 0.65 % (fine sand), and 0, 15.9 and 31.9 % (coarse sand) for 100, 200 and 300 cm^3 of distilled water, respectively. Results indicated different fly-ash behavior in various sands, as expected. While the fly-ash migrated freely thought the course sand, in the other two sands the fly-ash mobility decreased with decreasing grain sizes, e.g. pore sizes, which are documented on micromorphological images (Fig. 1). This is in agreement with the previous studies of *Gargiulo* et al. (2007), *Torkzaban* et al. (2008) and others.

The simulated final fly-ash distributions (Fig. 3) satisfactorily fitted observed data for all scenarios. Soil hydraulic parameters obtained from SGC3 scenario (Tab. 3) were sufficient to describe water flow from scenarios SGC1 and SGC2 for each sand. Interestingly the same longitudinal dispersivity, D_L, sticking efficiency, ζ, and the detachment coefficient, k_d, (Tab. 4) could be used not only for all 3 scenarios but also for all sands. Simulations for various sands differed only in the bulk density, ρ_d, and the diameters of the sand grains, d_c, (Tab. 4) which affected the attachment coefficients.

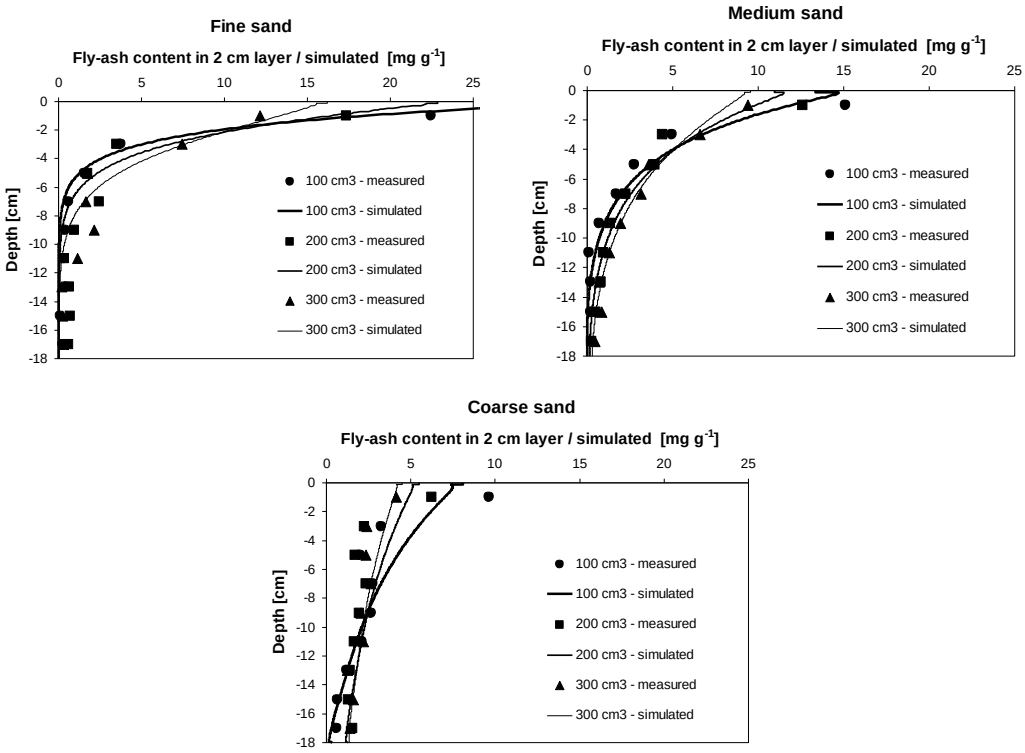

Fig. 2. Final fly-ash distribution measured in 2 cm thick sand layers and simulated using HYDRUS-1D in fine (top), medium (bottom left) and coarse (bottom right) sands packed in small glass cylinders.

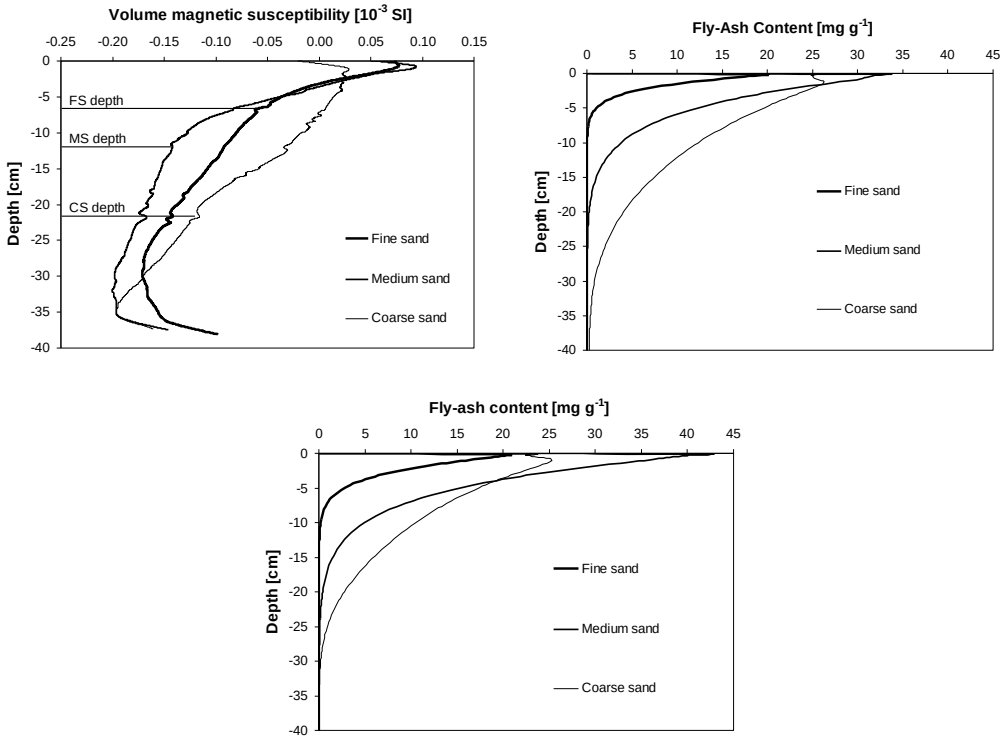

Fig. 3. Measured final volume magnetic susceptibilities (top left) indicating the maximum fly-ash concentrations (the peak values) and the fly-ash depths, and the final fly-ash distributions simulated using HYDRUS-1D in sands packed in large plastic cylinders using soil hydraulic parameters from the Tempe cells and small glass cylinder data (top right) and from the large plastic cylinder flow data (bottom).

Large columns

The final distributions of magnetic susceptibility within the sand columns packed in the large plastic cylinders are shown in Fig. 3. Measured magnetic susceptibility is in all cases highest at the top of the sand column due to the high content of fly-ash. As mentioned above, the magnetic susceptibilities were affected not only by the ferrimagnetic particles, but also by higher water content and temperature. However, despite the coincidental impact of all phenomena, the magnetic particles migration is indicated into the following depths: 7 cm in the fine sand, 12 cm in medium and 22 cm in coarse sand. The peak values indicated the depth of the highest fly-ash content within the sand columns. The lowest peak value of magnetic susceptibility was measured for the coarse sand due to the intensive migration of magnetic particles within the sand column.

Fly-ash behavior is also documented in the micromorphological images (Fig. 4). Thin sections were made from undisturbed sand samples polluted by fly-ash taken at the columns top after the experiments. While fly-ash migrated without significant restriction through the coarse sandy material (photo not shown), in the other two sands fly-ash is accumulated in few bottle neck pores. However, the fly-ash mobility was documented in both cases.

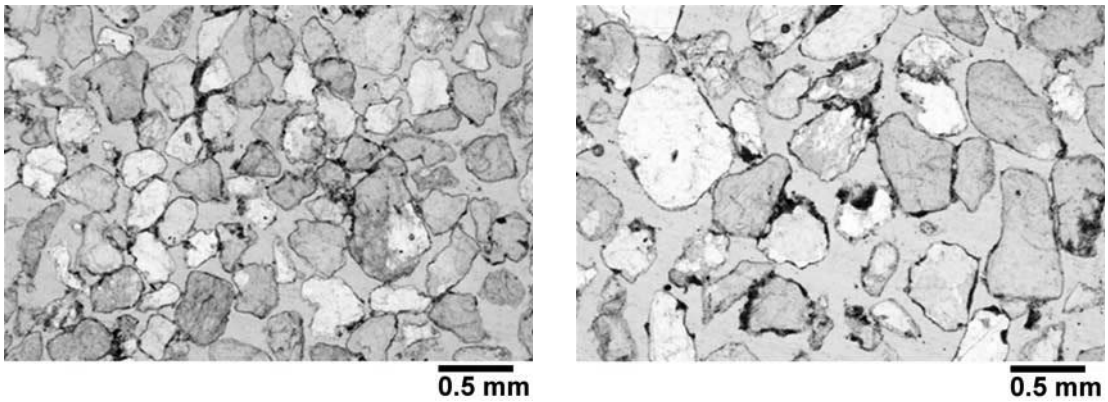

Fig. 4. Fly-ash distribution in fine (left) and medium (right) sands.

The final fly-ash distributions (Fig. 3) simulated using the average soil hydraulic parameters obtained from the large column data corresponded better to the indicated (by magnetic susceptibility) fly-ash distribution compare to that simulated using the parameters from the small column scenarios. Assuming SM400 sensor sensitivity, simulated data satisfactorily approximate the indicated peak values and the depths of fly-ash contamination.

In contrast to findings of other authors (summarized in *Gargiulo* et al., 2008), the model based on the filtration theory satisfactorily approximated observed fly-ash distribution in all cases. According to *Gargiulo* et al. (2008), recent studies have reported that the classical filtration theory is inadequate to describe colloid and bacteria deposition profiles when an energy barrier exists (unfavorable deposition conditions), and for larger sized colloids and finer texture media.

The colloid behavior in porous media strongly depends of on porous media and colloid surface properties. The ζ-potential, which is the most important, was measured for fly-ash suspension using ZetaPALS (Brookhaven Instrument Corporation, USA) and equaled to –10.08 mV. This value was considerably higher (closer to zero) compare to values measured for ultra fine fly-ash (varied between –15 and –40 mV and was lower for higher pH) by *Potgieter-Vermaak* et al. (2005) and indicates an incipient instability of the colloidal dispersion (for lower absolute value of ζ-potential attraction exceeds repulsion and dispersion flocculates). However, the fly-ash flocculation was not observed during the experiments probably mainly because all experiments were relatively short and suspension flow was fast. The ζ-potential of quartz grains was not measured because its measurement requires a different technique, which was not available. There are several studies, in which the ζ-potential of quartz grains was measured. *Johnsor* (1999) documented that the ζ-potential (–48 to –16 mV) increased with the increasing electrolyte ionic strength (10^{-5} to 10^{-1} M). *Elimelech* et al. (2000) showed that the ζ-potential (–24 to –80 mV) con-

siderably decreased with increasing pH (3 to 9) for 10^{-3} M NaCl used as a background electrolyte. *Saprykina* et al. (2010) cited considerably lower absolute value of the ζ-potential (–25.4 mV at pH 7.2). Grain coatings may significantly increase the ζ-potential value (even to the positive values) (*Elimelech* et al., 2000) and considerably influence (increase) colloid (which is negatively charged) attachment when studying colloid transport in sandy materials (*Shani* et al., 2008). No quartz grain coatings were expected in our study. The pH of water with sands was measured (7.25) and increased with fly-ash content (11.66, 12.4, 12.28, 12.34 and 12.38 for 10, 25, 50, 75 and 100 mg cm^{-3}, respectively). The other factor influencing the colloid attachment is a colloid and sand grain surface roughness and specific area. Sand grains were not round and smooth as is visible in Fig. 1. All these data and information indicated that conditions were slightly unfavorable for the fly-ash attachment to the sand grain. The numerical model success may be probably again contributed to the relatively simple course of the experiment (fast and short). Fly-ash was transported mainly during the sand sample saturation. No additional water was used to mobilize fly-ash particles.

Conclusions

The fly-ash migration within the sand columns of various particle size distributions was studied using different techniques. The experiments proved fly-ash mobility in studied sands. Visually observed and gravimetrically evaluated fly-ash migration in the small glass cylinders corresponded to the fly-ash mobility in the large columns detected magnetically using the SM400. Fly-ash mobility strongly depended on the sand particle size distribution. While the fly-ash migrated freely through the coarse sand, in the other two sands the fly-ash migration decreased with the decreasing sand particle sizes. Water flow and fly-ash transport was simulated using the HYDRUS-1D code. Sand particle distribution influenced porous system, hydraulic properties and consequently water flow intensity. Particle sizes and pore water velocity influenced the first-order deposition (attachment) coefficient, which was calculated assuming filtration theory. The other parameters (longitudinal dispersivity, sticking efficiency and the detachment coefficient) characterizing fly-ash transport were the same for all three sands. Simulated fly-ash distribution within the sands columns satisfactorily approximated observed and indicated data.

Acknowledgement: Authors acknowledge the financial support of the Grant Agency of Academy of Sciences of the Czech Republic grant No. A300120701, and the Ministry of Education, Youth and Sports grant No. MSM 6046070901. We also thank to Anna Žigová for taking micromorphological images. Our thanks are also to Vladana Ciprýnová for her help with the sand selection and to sand mine Sklopísek Střeleč that generously supplied us by 500 kilograms of technical sands.

List of symbols

θ – water content [$L^3 L^{-3}$],
θ_e – effective soil water content [–],
θ_r – residual soil water contents [$L^3 L^{-3}$],
θ_s – saturated soil water contents [$L^3 L^{-3}$],
h – pressure head [L],
l – pore-connectivity parameter [–],
α – parameter [L^{-1}],
n – parameter [–],
m – parameter [–],
K – hydraulic conductivity [$L T^{-1}$],
K_s – saturated hydraulic conductivity [$L T^{-1}$],
c – (colloid, virus, bacteria) concentration in the aqueous phase [$M L^{-3}$],
s – solid phase (colloid, virus, bacteria) concentration [$M M^{-1}$],
ρ_d – bulk density [$M L^{-3}$],
k_a – first-order deposition (attachment) coefficient [T^{-1}],
k_d – first-order entrainment (detachment) coefficient [T^{-1}],
ψ – colloid retention function [–],
d_c – diameter of the sand grains [L],
d_{co} – diameter of the colloid particles [L],
ζ – sticking efficiency [–],
v – pore-water velocity [$L T^{-1}$],
η – single-collector efficiency [–],
D_L – longitudinal dispersivity [L],
m_t – final fly-ash content in soil columns [$M M^{-1}$].

REFERENCES

AUSET M., KELLER A.A., 2004: Pore-scale processes that control dispersion of colloids in saturated porous media. Water Resour. Res., *40*, W03503, doi: 10.1029/2003WR002800.

BOLSTER C.H., MILLS A.L., HORNBERGER G.M., HERMAN J.S., 1999: Spatial distribution of bacteria experiments in intact cores. Water Resour. Res., *35*, 1797–1807.

BOYKO T., SCHOLGER R., STANEK H., 2004. Topsoil magnetic susceptibility mapping as a tool for pollution monitoring: repeatability of in situ measurements. J. Appl. Geophys., *55*, 3-4, 249–259.

BRADFORD S.A., BETTAHAR M., SIMUNEK J., VAN GENUCHTEN M.T., 2004: Straing and attachment of colloids in physically heterogeneous porous media. Vadose Zone J., 3, 384–394.

BRADFORD S.A., SIMUNEK J., BETTAHAR M., TADASSA Y.F., VAN GENUCHTEN M.T., YATES S.R., 2005: Straing of colloids at textural interfaces. Water Resour. Res., *41*, 10, W10404.

BRADFORD S.A., SIMUNEK J.,BETTAHAR M., VAN GENUCHTEN M.T., YATES S.R., 2003: Modelling colloid attachment, straining, and exclusion in saturated porous media. Environ.Sci. Technik., *37*, 2242–2250.

BRADFORD S.A., YATES S.R. BETTAHAR M., SIMUNEK J., 2002: Physical factors affecting the transport and fate of colloids in saturated porous media. Water Resour. Res., *38*, 1327, doi: 10.1029/2002WR001340.

DELTA-T DEVICES LTD., 2005: User Manual for the Moisture Meter, type HH2, Cambridge.

ELIMELECH M., NAHI M., KO C.-H., RYAN J.N., 2000: Relative insignificance of mineral grain zeta potential to colloid transport in geochemically heterogeneous porous media. Environ. Sci. Technol., *34*, 2143–2148.

FLANDERS P.J., 1994: Collection, measurements and analysis of airborne magnetic particulates from pollution in the environment. J. Appl. Phys., *75*, 5931–5936.

FOPPEN J.W., LUTTERODT G., ROLING F.M., UHLENBROOL S., 2010: Towards understanding inter-strain attachment variations of Escherichia coli during transport in saturated quartz sand. Water Res., *44*, 1202–1212.

GAO H., QIU C.Q., FAN D.M., JIM Y., WANG L.P., 2010: Three-dimensional microscale flow simulations and colloid transport modeling in saturated soil porous media. Computer and Mathematics with Applications, *59*, 7, 2271– –2289.

GARGIULO G., BRADFORD S., ŠIMŮNEK J., USTOHAL P., VEREEKER H., KLUMPP E., 2007: Bacteria transport and deposition under unsaturated conditions: The role of the matrix grain size and the bacteria surface proteins. J. Contam. Hydrol., *92*, 255–273.

GARGIULO G., BRADFORD S., ŠIMŮNEK J., USTOHAL P., VEREEKER H., KLUMPP E., 2008: Bacteria transport and deposition under unsaturated conditions: The role of water content and bacteria surface hydrophobicity. Vadose Zone J., *7*, 2, 406–419.

HAY K.L., DEARING J.A., BABAN S.M.J., LOVELAND P.J., 1997: A preliminary attempt to identify atmospherically-derived pollution particles in English topsoils from magnetic susceptibility measurements. Phys. Chem. Earth, *22*, 207–210.

HELLER F., STRZYSZCZ Z., MAGIERA T., 1998: Magnetic record of industrial pollution in forest soils of Upper Silesia, Poland. J. Geophys. Res., *103*, 17767–17774.

HANESCH M., SCHOLGER R., 2002: Mapping of heavy metal loadings in soils by means of magnetic susceptibility measurements. Environ. Geology, *42*, 8, 857–870.

HANESCH M., SCHOLGER R., REY D., 2003: Mapping dust distribution around an industrial site by measuring magnetic parameters of tree leaves. Atm. Environment, *37*, 5125– –5133.

JIANG S., PANG L., BUCHAN G.D., ŠIMŮNEK J., NOONAN M.J., CLOSE M.E., 2010: Modeling water flow and bacterial transport in undisturbed lysimeters under irrigations of dairy shed effluent and water using HYDRUS-1D. Water Res., *44*, 1050–1061.

JOHNSOR P.R. 1999: A comparison of streaming and microelectrophoresis methods for obtaining the ζ potential of granular porous media surfaces. J. of Colloid and Interface Science, 209, 264–267.

KAPIČKA A., JORDANOVA N., PETROVSKÝ E., USTJAK S., 2001: Effect of different soil conditions on magnetic parameters of power-plant fly ashes J. Appl. Geophys., *48*, 93–102.

KAPIČKA A., KODEŠOVÁ R., PETROVSKÝ E., HŮLKA Z., GRISON H., KAŠKA M., 2011: Experimental study of fly-ash migration by using a magnetic method. Studia Geoph. Geod., *55*, in print.

KAPIČKA A., PETROVSKÝ E., FIALOVÁ H., PODRÁZSKÝ V., DVOŘÁK I., 2008: High resolution mapping of anthropogenic pollution in the Giant Mountains National Park using soil magnetometry. Studia Geoph. Geod., *52*, 271–284.

KAPIČKA A., PETROVSKÝ E., USTJAK S. and MACHÁČKOVÁ, K., 1999: Proxy mapping of fly-ash pollution of soils around a coal-burning power plant: a case study in the Czech Republic, J. Geoch. Explor., *66*, 291– –297.

KELLER A.A., SIRIVITHAYAPAKORN S., CHRYSIKOPOULOS V., 2004: Early breakthrough of colloids and bacteriophage MS2 in a water-saturated sand column, Wat. Resour. Res., *40*, W08304, doi:10.1029/2003WR002676.

KIM S.B., 2006: Numerical analysis of bacteria transport in saturated porous media. Hydrol. Proc., *20*, 5, 1177–1186.

MAGIERA T., STRZYSZCZ Z., 2000: Ferrimagnetic minerals of anthropogenic origin in soils of some polish national parks. Water, Air and Soil Pollution, *124*, 37–48.

PETROVSKÝ E., ELLWOOD B.B., 1999. Magnetic monitoring of air-land and water-pollution. In: Quaternary Climates, Environments and Magnetism (B.A. Maher, R. Thompson, Eds.), Cambridge Univ. Press.

PETROVSKÝ E., HŮLKA Z., KAPIČKA A., MAGPROX TEAM, 2004: New tool for in-situ measurements of vertical distribution of magnetic susceptibility in soils as basis for mapping deposited dust. Environ. Technol., *25*, 1021–1029.

POTGIETER-VERMAAK S.S., POTGIETER J.H., KRUGER R.A., SPOLNIK Z., VAN GRIEKEN R., 2005: A characterization of the surface properties of an ultra fine fly ash (UFFA) used in the polymer industry. Fuel, *84*, 2295–2300.

SAPRYKINA M.N., YAROSHEVSKAYA N.V., SAVCHINA L.A., GONCHARUK V.V., 2010: Adhesion analysis of micromycetes on granular media. J. Water Chem. Technol., *32*, 284–289.

SHANI C., WEISBROD N., YAKIREVICH A., 2008: Colloid transport through saturated sand columns: Influence of physical and chemical surface properties on deposition. Colloids and Surfaces A: Physicochem. Eng. Aspects, *316*, 142–150.

SHARMA A.P., TRIPATHI B.D., 2008: Magnetic mapping of fly-ash pollution and heavy metals from soil samples around a point source in a dry tropical environment. Environmental Monitoring and Assessment, *138*, 31–39.

SCHINNER T., LETZNER A., LIEDTKE S., CASTRO F.D., EYDELNANT I.A., TUFENKJI N., 2010: Transport of selected bacteria pathogens in agricultural soil and quartz sand. Water Res., *44*, 1182–1192.

SIM Y., CHRYSIKOPOULOS V., 2000: Virus transport in unsaturated porous media. Wat. Resour. Res., *36*, 173–179.

SIRIVITHAYAPAKORN S., KELLER A.A., 2003: Transport of colloids in unsaturated porous media: A pore-scale observation of processes during the dissolution of air-water interface, Wat. Resour. Res., *39*, 12, 1346, doi: 10.1029/2003WR002487.

ŠIMŮNEK J., ŠEJNA M., SAITO H., SAKAI M., VAN GENUCHTEN M. TH., 2008a: The HYDRUS-1D Software Package for Simulating the Movement of Water, Heat, and Multiple Solutes in Variably Saturated Media, Version 4.0, HYDRUS Software Series 3, Department of Environmental Sciences, University of California Riverside, Riverside, California, USA, pp. 315.

ŠIMŮNEK J., VAN GENUCHTEN M. TH., 2008b: Modeling nonequilibrium flow and transport with HYDRUS, Vadose Zone J., *7*, 2, 782–797.

SPITERI C., KALINSKI V., ROSLER W., HOFFMANN V., APPEL E., MAGPROX TEAM, 2005: Magnetic screening of a pollution hotspot in the Lausitz area, Eastern Germany: correlation analysis between magnetic proxies and heavy metal contamination in soils. Environmental Geology, *49*, 1–9.

TORKZABAN S., TAZEHKAND S.S., WALKER S.L., BRADFORD S.A. 2008: Transport and fate of bacteria in porous media: Coupled effects of chemical conditions and pore space geometry. Wat. Resour. Res., *44*, 4, W04403.

UMS GMBH, MUNICH, 2005: T5 Miniature Pressure Transducer Tensiometer, User Manual version 1.8, Munich.

VAN GENUCHTEN M. TH., 1980: A closed-form equation for predicting the hydraulic conductivity of unsaturated soils. Soil Sci. Soc. Am. J., *44*, 892–898.

VAN GENUCHTEN M., TH., ŠIMŮNEK J., LEIJ F.J., ŠEJNA M.. 2005: RETC, Version 6.02, Code for Quantifying the Hydraulic Functions of Unsaturated Soils, http://www.pc-progress.com/en/Default.aspx?retc-downloads.

WOSSNER W.W., BALL P.N., DEBORDE D.C., TROY T.L., 2001: Viral transport in a sand and gravel aquifer under field pumping conditions. Ground Water, *39*, 886–894.

ZHANG W., BROWN G.O., STORM D.E., ZHANG H., 2008: Fly-ash-amended sand as filter media in bioretention cells to improve phosphorus removal. Wat. Environ. Res., *80*, 6, 507–516.

Received 28 January 2011
Accepted 12 April 2011